Pao et al. EURASIP Journal on Wireless Communications and Networking (2017) 2017:163
DOI 10.1186/s13638-017-0945-9

EURASIP Journal on Wireless Communications and Networking

RESEARCH Open Access

Joint ABS and user grouping allocation for HetNet with picocell deployment in downlink

Wei-Chen Pao[1], Jhih-Wei Lin[2], Yung-Fang Chen[2*] and Chin-Liang Wang[3]

Abstract

In order to resolve the co-channel inter-cell interference problem in heterogeneous networks (HetNet), the feature of almost blank subframes (ABS) in the time domain of the enhanced inter-cell interference coordination (eICIC) is utilized. In this paper, an ABS configuration design is developed on downlink in HetNet and the associated resource allocation problem for maximizing the system performance with fairness among user equipments (UEs) is considered. Compared to conventional problems, the resource assignment problems include the configuration of ABS pattern and the resource allocation for macro UEs and pico UEs, which aims to maximize the downlink throughput and balance the traffic offloading in intra-frequency HetNet deployments. First, this paper introduces an ABS pattern design by using the channel condition, which is developed in terms of the time domain resource. Subframes are categorized as protected or normal subframes for reducing interference impact to pico UEs. Based on the configuration of the ABS pattern, we develop a grouping strategy to determine which pico UEs use either protected or normal subframes. Besides, the assignment of resource blocks with respect to the resource in the frequency domain is developed along with the fairness among UEs. The proposed joint allocation scheme takes the system throughput and the fairness into account, and has better performance than the existing schemes. Simulation results also reveal that the performance of the proposed joint allocation scheme approximates the optimal solution with the full search scheme.

Keywords: Inter-cell interference coordination, Almost blank subframe, Heterogeneous network, Proportional fairness, Resource allocation

1 Introduction

Orthogonal frequency division multiple access (OFDMA) system has been chosen for the next-generation broadband wireless system standards [1] in order to satisfy the growing demands on the high data traffic in the mobile communication systems. The Third Generation Partnership Project (3GPP) Long Term Evolution (LTE) has been regarded as a promising mobile technology with increased system sum rates [2]. The LTE-Advanced (LTE-A) is an evolution of LTE, which achieves International Mobile Telecommunications (IMT)-Advanced requirements [3–5]. With more data traffic demand in the future, enhancing the system spectral efficiency by the deployment of traditional macro eNodeBs (eNBs) has high cost. Therefore, heterogeneous networks (HetNet) have been widely discussed in 3GPP LTE-A standards [6, 7]. HetNet includes high-power macro eNBs and low-power nodes, such as femto eNBs, pico eNBs, and relays [8–10].

In order to offload user equipments (UEs) from a macro eNB to a pico eNB more efficiently, cell range expansion (CRE) has been introduced in 3GPP LTE-A [11]. In the CRE method, a bias value is introduced and added to reference signal received power (RSRP) of pico eNBs. A CRE region is introduced where the system pretends that UEs have better signal quality from the pico eNB. Therefore, the system may tend to offload UEs from the macro eNB to the pico eNB. More UEs may connect to pico eNBs for load balancing. The control of the bias and the related offloading is discussed in [12, 13]. However, the UE which is handed over from the macro eNB to the pico eNB with the CRE technique may suffer severe interference from the macro eNB since the received signal from

* Correspondence: yfchen@ce.ncu.edu.tw
[2]Department of Communication Engineering, National Central University, Taoyuan, Taiwan, Republic of China
Full list of author information is available at the end of the article

pico eNB is still weak. A major problem in HetNet [14] is the cross-tier inter-cell interference (ICI) because the low-power nodes such as pico eNBs share the same frequency band with the macro eNBs. In order to improve the performance and reduce the cross-tier interference, a major feature of enhanced inter-cell interference coordination (eICIC) [10, 15–18] is to coordinate inter-cell interference in time domain by implementing almost blank subframe (ABS). The method of time-domain multiplexing (TDM) using ABS [19, 20] is introduced to avoid heavy ICI on both data and control channels of the downlinks. When the ABS scheme is employed, subframes will be further configured as either normal subframes or protected subframes. For normal subframes, UEs served by macro eNBs (macro UEs) and served by pico eNBs (pico UEs) are all allowed to use these subframes. For protected subframes, only pico UEs are allowed to use those subframes. The designs of the CRE region and the ABS pattern can be developed to have gain and benefit for the whole system, such as traffic offloading and throughput.

Regarding the above discussion, we focus on the challenges for maximizing the system performance with fairness among UEs in HetNet which include the configuration design of the ABS pattern and the resource allocation for macro UEs and pico UEs in terms of the time domain resource, i.e., subframe configuration including protected subframe and normal subframe where the resource is located in the time domain, and the frequency domain resource, i.e., subcarrier allocation to multiple UEs where this resource is located in the frequency domain. Due to the design of the CRE region and ABS to protect Pico UEs, the resource allocation problem becomes more complicated. The ABS pattern needs to be configured and coordinated among eNBs for the purpose of the maximization of system capacity or throughput. Also, subcarriers should be properly assigned to macro UEs and Pico UEs. The associated configuration, i.e., a normal or a protected subframe of a particular subcarrier will determine the amount of the suffered interference. We also consider fairness among Pico UEs. Consequently, the proposed resource allocation scheme comprises the ABS configuration, the Pico UE grouping, and the subcarrier allocation.

First, this paper focuses on the design for the configuration of an ABS pattern. The problems of cell selection combined with ABS density are investigated in [21–23]. The channel state is usually assumed to be time invariant in the period of an ABS pattern [24, 25]. Thus, most of papers only discuss the ABS density without determining which subframes should be configured as protected subframes. The system performance, e.g., throughput, is affected by the ABS configuration since each subcarrier or each UE experiences different channel condition. In the view of the time domain, the ABS pattern design strategy is developed. We utilize the channel condition to design an evaluation function as an indicator which aims to maximize the sum rate of the system. The indicator can efficiently determine which subframes should be configured as protected subframes. Different from the previous work [22], the ABS pattern is dynamically adjusted, instead of fixed.

Second, this paper develops a pico UE grouping strategy based on an optimization technique to determine which pico UEs use protected subframes or normal subframes. Various schemes of pico UE grouping [24–27] have been investigated in the HetNet with CRE. The simplest way is that all pico UEs are assigned to use protected subframes [26], which means pico eNBs only work in protected subframes. This scheme may cause the reduced performance in pico eNBs due to the limited resources. In [27], some pico UEs which are handovered from a macro eNB to a pico eNB with the CRE technique are assigned to the protected UE set and others are assigned to the normal UE set. In [25], "brute force search" by employing integer programming is used to get the optimal solution for the problem of the time-domain resource partitioning for enhanced inter-cell interference coordination. However, this scheme has a high computational complexity. In order to reduce the computational complexity, one scheme [24] using Nash bargaining solution (NBS) is proposed to reduce the complexity, but the NBS scheme only finds a sub-optimal solution in some sense. Therefore, it raises our motivation to develop a pico UE grouping scheme with a low computational complexity while approximating the optimal solution. We also develop a strategy for the pico UE grouping to determine which pico UEs use either the normal subframes or the protected subframes. Deviated from the tradition UE grouping methods [28–30], Pico UEs will be re-distributed by using a fast adjustment in a group basis and a refinement mechanism on a per-UE basis. Accompanied by the re-distribution, the radio resource blocks in the frequency domain are allocated jointly per subframe.

Finally, in this paper, we propose joint allocation scheme to maximize the system performance while considering fairness among UEs by appending some processing procedures. A dynamic ABS pattern design is introduced. Based on the ABS pattern, UE grouping strategies including the fast adjustment and the refinement mechanism are introduced. Meanwhile, the radio resource allocation is executed as well. The proposed scheme outperforms the existing schemes [24, 27] and approaches the full search scheme [25] while the computational complexity is greatly reduced. The proposed algorithm is different from other works, such as (1) time-domain resource portioning [23, 24, 27] without user grouping or subcarrier allocation, (2) fair scheduling [31, 32] without ABS configuration and user grouping, or (3) user selection and resource allocation algorithm [33] without ABS configuration.

Our contributions and new ideas include (a) a joint allocation scheme is first developed in the time domain and the frequency domain, including the consideration of the proportional fairness among UEs; (b) a new evaluation function based on an optimization technique is proposed to determine the configuration of subframes, i.e., normal and protected subframes. A low complexity associated strategy is thus proposed; (c) another new evaluation function is derived for UE grouping, i.e., in either the normal or the protected UE set; (d) the proposed scheme outperforms the existing schemes [24, 27], and approaches the optimal solution with the full search scheme [25].

2 System model and problem formulation

We consider a downlink transmission scenario of the two-tier cellular network in an OFDMA system, which consists of one macro eNB and one pico eNB. The HetNet deployment including a pico eNB within the coverage of a macro eNB is depicted in Fig. 1. In the cell range expansion (CRE) [11] technique, a bias value is introduced and added to reference signal received power (RSRP) of pico eNBs. The numbers of UEs served by the macro eNB and the pico eNB are denoted by $K^{'}$ and $K^{''}$, respectively. The corresponding UE sets are $\Omega^{(\text{Macro})}$ and $\Omega^{(\text{Pico})}$. All K UEs ($K = K^{'} + K^{''}$) are uniformly distributed within the coverage of the macro eNB. Each UE is only allowed to connect a single eNB. The serving eNB for the kth UE is determined by comparing the values of RSRP [29, 30]. The kth UE chooses the pico eNB with a bias if the following holds true:

$$\text{RSRP}_k^{(\text{Pico})} + \text{bias} \geq \text{RSRP}_k^{(\text{Macro})} \tag{1}$$

where $\text{RSRP} = p_r \cdot |G|^2$. G means the channel gain and p_r means the reference signal power per resource element [29]. bias (in dB) is chosen to be a positive value toward pico eNBs. Otherwise, the kth UE is served by the macro eNB.

The offloaded UEs in the CRE region may suffer from ICI of macro eNBs. In normal subframes, macro UEs and pico UEs are all allowed to use those subframes. In this paper, pico UEs will be further classified into two sets, a normal UE set $\Omega^{(\text{normal})}$ and a protected UE set $\Omega^{(\text{protected})}$. UEs in the normal UE set use the normal subframes, and UEs in the protected UE set use the protected subframes. We also assume that the same ABS patterns are configured for all eNBs under consideration, which is the synchronous configuration of ABS pattern [34] as shown in Fig. 1. An ABS pattern means the pattern of the protected subframes in a frame. The channel state information is known to eNBs and the information of ABS configuration exchanges through X2 interface between all eNBs in LTE [19].

We assume that the system has N resource blocks (RBs) and each RB includes Q subcarriers. For pico UEs, the signal to interference plus noise ratio (SINR) for the

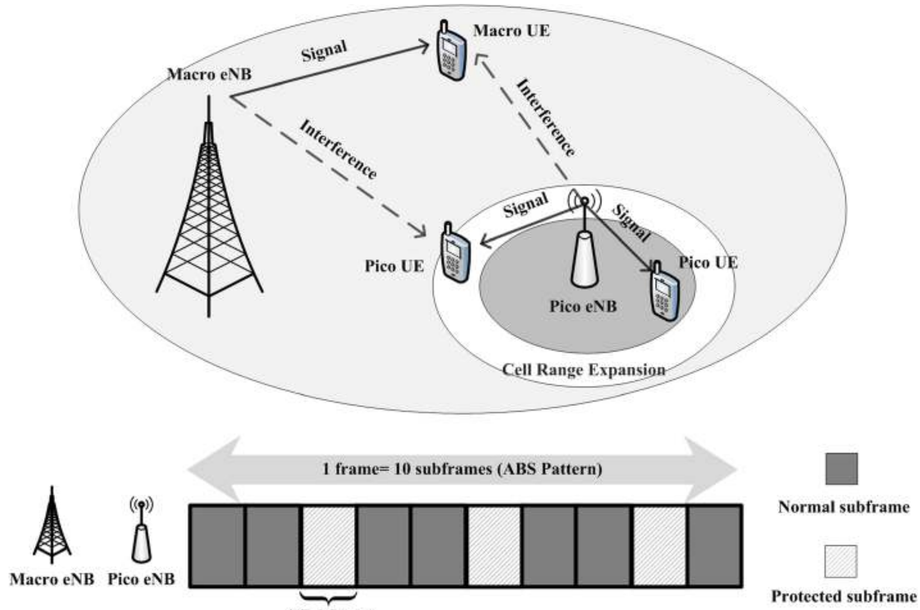

Fig. 1 Heterogeneous network with inter-cell interference and cell range expansion

k''th pico UE on the qth subcarrier of the nth RB at the ith subframe can be expressed as:

$$\mathrm{SINR}^{(\mathrm{Pico})}_{k'',n,q}[i] = \frac{\left|G^{(\mathrm{Pico})}_{k'',n,q}[i]\right|^2 p^{(\mathrm{Pico})}_{k'',n,q}[i]}{N_0\Delta f + \left|G^{(\mathrm{Macro})}_{k'',n,q}[i]\right|^2 \varepsilon[i] p^{(\mathrm{Macro})}_{k',n,q}[i]} \quad (2)$$

where i is the subframe index; $G^{(\mathrm{Pico})}_{k'',n,q}[i]$denotes the channel gain between the pico eNB and the k''th pico UE on the qth subcarrier of the nth RB; $p^{(\mathrm{Pico})}_{k'',n,q}[i]$ is the amount of power for the k''th pico UE on the qth subcarrier of the nth RB; N_0 is the AWGN noise power spectral density; $\Delta f$is the subcarrier spacing; $G^{(\mathrm{Macro})}_{k'',n,q}[i]$ denotes the channel gain between the macro eNB and the k''th pico UE on the qth subcarrier of the nth RB; $p^{(\mathrm{Macro})}_{k',n,q}[i]$ is the amount of power for the k'th macro UE on the qth subcarrier of the nth RB; $\varepsilon[i]$denotes the binary indicator; $\varepsilon[i] = 1$represents that the ith subframe is the normal subframe; $\varepsilon[i] = 0$represents that the ith subframe is the protected subframe.

In the frequency domain, the basic resource allocation unit for scheduling is the RB unit. In the time domain, resource allocation scheduling is performed based on the subframe unit. Therefore, the data rate for the k''th pico UE on the nth RB at the ith subframe can be expressed as:

$$\begin{aligned} r^{(\mathrm{Pico})}_{k'',n}[i] &= \sum_{q=1}^{Q} \Delta f \log_2\left(1 + SINR^{(\mathrm{Pico})}_{k'',n,q}[i]\right) \\ &= \begin{cases} r^{(\mathrm{normal})}_{k''}[i], k'' \in \Omega^{(\mathrm{normal})} \\ r^{(\mathrm{protected})}_{k''}[i]\ k'' \in \Omega^{(\mathrm{protected})} \end{cases} \end{aligned} \quad (3)$$

where $r^{(\mathrm{normal})}_{k'',n}[i]$and $r^{(\mathrm{protected})}_{k'',n}[i]$ are the data rate for the k''th pico UE on the nth RB in the normal UE set and the protected UE set, respectively.

The sum of the data rate for the k''th pico UE at the ith subframe can be expressed as:

$$\begin{aligned} R^{(\mathrm{Pico})}_{k''}[i] &= \sum_{n=1}^{N} \rho^{(\mathrm{Pico})}_{k'',n}[i] r^{(\mathrm{Pico})}_{k'',n}[i] \\ &= \sum_{n=1}^{N} \rho^{(\mathrm{Pico})}_{k'',n}[i] \sum_{q=1}^{Q} \Delta f \log_2\left(1 + SINR^{(\mathrm{Pico})}_{k'',n,q}[i]\right) \\ &= \begin{cases} R^{(\mathrm{normal})}_{k''}[i], k'' \in \Omega^{(\mathrm{normal})} \\ R^{(\mathrm{protected})}_{k''}[i]\ k'' \in \Omega^{(\mathrm{protected})} \end{cases} \end{aligned} \quad (4)$$

where $\rho^{(\mathrm{Pico})}_{k'',n}[i]$ denotes the binary indicator. $\rho^{(\mathrm{Pico})}_{k'',n}[i] = 1$ represents that the nth RB is assigned to the k''th pico UE. $R^{(\mathrm{normal})}_{k''}[i]$ and $R^{(\mathrm{protected})}_{k''}[i]$ are the sum of data rate for the k''th pico UE in the normal UE set and the protected UE set, respectively. Note that, if the ith subframe is normal, $R^{(\mathrm{normal})}_{k''}[i]$ is evaluated and $R^{(\mathrm{protected})}_{k''}[i]$ equals 0. Similarly, for macro UEs, the SINR for the k'th macro UE on the qth subcarrier of the nth RB at the ith subframe can be expressed as:

$$\mathrm{SINR}^{(\mathrm{Macro})}_{k',n,q}[i] = \frac{\left|G^{(\mathrm{Macro})}_{k',n,q}[i]\right|^2 \varepsilon[i] p^{(\mathrm{Macro})}_{k',n,q}[i]}{N_0\Delta f + \left|G^{(\mathrm{Pico})}_{k',n,q}[i]\right|^2 p^{(\mathrm{Pico})}_{k'',n,q}[i]} \quad (5)$$

The data rate for the k'th macro UE on the nth RB at the ith subframe can be expressed as:

$$r^{(\mathrm{Macro})}_{k',n}[i] = \sum_{q=1}^{Q} \Delta f \log_2\left(1 + SINR^{(\mathrm{Macro})}_{k',n,q}[i]\right). \quad (6)$$

The sum of the data rate for the k'th macro UE at the ith subframe can be expressed as:

$$\begin{aligned} R^{(\mathrm{Macro})}_{k'}[i] &= \sum_{n=1}^{N} \rho^{(\mathrm{Macro})}_{k',n}[i] r^{(\mathrm{Macro})}_{k',n}[i] \\ &= \sum_{n=1}^{N} \rho^{(\mathrm{Macro})}_{k',n}[i] \sum_{q=1}^{Q} \Delta f \log_2\left(1 + SINR^{(\mathrm{Macro})}_{k',n,q}[i]\right) \end{aligned} \quad (7)$$

where $\rho^{(\mathrm{Macro})}_{k',n}[i]$ denotes the binary indicator. $\rho^{(\mathrm{Macro})}_{k',n}[i] = 1$ represents that the nth RB is assigned to the k'th macro UE. Therefore, the sum rate of the system is known as $\sum_{i=1}^{I}\left\{\sum_{k'=1}^{K'} R^{(\mathrm{Macro})}_{k'}[i] + \sum_{k''=1}^{K''} R^{(\mathrm{Pico})}_{k''}[i]\right\}$.

Our goal is to maximize the system performance subject to the transmit power constraints while considering the fairness among all UEs [31, 32]. The resource allocation problem for the time domain eICIC is formulated as:

$$\begin{aligned} \max_{\varepsilon[i],\varepsilon^*[i],C_{k''},C^*_{k''}} & \left\{\sum_{i=1}^{I}\left(\sum_{k'=1}^{K'} \frac{\varepsilon[i] R^{(\mathrm{Macro})}_{k'}[i]}{\overline{R}^{(\mathrm{Macro})}_{k'}[i]} + \sum_{k''=1}^{K''} \frac{\varepsilon[i] C_{k''} R^{(\mathrm{normal})}_{k''}[i]}{\overline{R}^{(\mathrm{Pico})}_{k''}[i]} \right.\right. \\ & \left.\left. + \sum_{k''=1}^{K''} \frac{\varepsilon^*[i] C^*_{k''} R^{(\mathrm{protected})}_{k''}[i]}{\overline{R}^{(\mathrm{Pico})}_{k''}[i]}\right)\right\} \\ = & \left\{\sum_{i=1}^{I}\left(\sum_{k'=1}^{K'} \frac{\varepsilon[i]}{\overline{R}^{(\mathrm{Macro})}_{k'}[i]} \sum\nolimits_{n=1}^{N} \rho^{(\mathrm{Macro})}_{k',n}[i] r^{(\mathrm{Macro})}_{k',n}[i] \right.\right. \\ & + \sum_{k''=1}^{K''} \frac{\varepsilon[i] C_{k''}}{\overline{R}^{(\mathrm{Pico})}_{k''}[i]} \sum_{n=1}^{N} \rho^{(\mathrm{Pico})}_{k'',n}[i] r^{(\mathrm{normal})}_{k'',n}[i] \\ & \left.\left. + \sum_{k''=1}^{K''} \frac{\varepsilon^*[i] C^*_{k''}}{\overline{R}^{(\mathrm{Pico})}_{k''}[i]} \sum_{n=1}^{N} \rho^{(\mathrm{Pico})}_{k'',n}[i] r^{(\mathrm{protected})}_{k'',n}[i]\right)\right\} \end{aligned} \quad (8)$$

subject to

$$\sum_{k^{'}\in\Omega^{(\mathrm{Macro})}}\sum_{n=1}^{N}\sum_{q=1}^{Q}p_{k^{'},n,q}^{(\mathrm{Macro})}[i]\leq P^{(\mathrm{Macro})}[i] \quad (9)$$

$$\sum_{k^{''}\in\Omega^{(\mathrm{Pico})}}\sum_{n=1}^{N}\sum_{q=1}^{Q}p_{k^{''},n,q}^{(\mathrm{pico})}[i]\leq P^{(\mathrm{Pico})}[i] \quad (10)$$

$$\sum_{k^{'}=1}^{K^{'}}\rho_{k^{'},n}^{(\mathrm{Macro})}[i]=1,\ \ \mathrm{for}\ n=1,\ldots,N \quad (11)$$

$$\sum_{k^{''}=1}^{K^{''}}\rho_{k^{''},n}^{(\mathrm{Pico})}[i]=1,\ \ \mathrm{for}\ n=1,\ldots,N \quad (12)$$

$$\varepsilon[i]+\varepsilon^{*}[i]=1 \quad (13)$$

$$C_{k^{''}}+C_{k^{''}}^{*}=1 \quad (14)$$

where the first term of Eq. (8) is the feasible rate relative to its current average data rate of the macro UEs coupled with the average data rate $\overline{R}_{k^{'}}^{(\mathrm{Macro})}[i]$ of the $k^{'}$th macro UE; the second term of Eq. (8) is the feasible rate relative to its current average data rate of the pico UEs which are in the normal UE set coupled with the average data rate $\overline{R}_{k^{''}}^{(\mathrm{Pico})}[i]$ of the $k^{''}$th pico UE; the third term of Eq. (8) is the feasible rate relative to its current average data rate of the pico UEs which are in the protected UE set coupled with the average data rate $\overline{R}_{k^{''}}^{(\mathrm{Pico})}[i]$ of the $k^{''}$th pico UE; the average data rate for macro UEs and pico UEs is defined as:

$$\overline{R}^{k^{'}(\mathrm{Macro})}[i+1]=\left(1-\frac{1}{JI}\right)\overline{R}_{k^{'}}^{(\mathrm{Macro})}[i]+\frac{1}{JI}R_{k^{'}}^{(\mathrm{Macro})}[i] \quad (15)$$

and

$$\overline{R}_{k^{''}}^{(\mathrm{Pico})}[i+1]=\left(1-\frac{1}{JI}\right)\overline{R}_{k^{''}}^{(\mathrm{Pico})}[i]+\frac{1}{JI}R_{k^{''}}^{(\mathrm{Pico})}[i]. \quad (16)$$

$1/\overline{R}_{k^{'}}^{(\mathrm{Macro})}[i]$ and $1/\overline{R}_{k^{''}}^{(\mathrm{Pico})}[i]$ in Eq. (8) are the proportional fairness (PF) factors which are introduced to strike a balance between the system performance and the fairness among UEs [32]; i is the subframe index; $I$is the number of subframes in one frame; J is the window size which is the number of the frames in a PF period; $\varepsilon[i]$and $\varepsilon^{*}[i]$are the binary indicators; $\varepsilon[i]=1$ ($\varepsilon^{*}[i]=0$) represents that the ith subframe belongs to the normal subframe; $\varepsilon^{*}[i]=1$ ($\varepsilon[i]=0$) represents that the ith subframe belongs to the protected subframe; $C_{k^{''}}$ and$C_{k^{''}}^{*}$ denote the indicators for the UE $k^{''}$ whether it is assigned to the normal UE set or the protected UE set. $C_{k^{''}}=1$ ($C_{k^{''}}^{*}=0$) represents that the $k^{''}$th pico UE is assigned to the normal UE set; $C_{k^{''}}^{*}=1$ ($C_{k^{''}}=0$) represents that the $k^{''}$th pico UE is assigned to the protected UE set; Eq. (9) represents that the sum of the allocated power $p_{k^{'},n,q^{(\mathrm{Macro})}}[i]$ is less than the total power of the macro eNB$P^{(\mathrm{Macro})}[i]$; Eq. (10) represents the transmit power constraint of the pico eNB $P^{(\mathrm{Pico})}[i]$; Eq. (11) denotes that each RB in the macro eNB is only allocated to one macro UE; each RB in one eNB is not allowed to be shared among UEs served in the eNB; Eq. (12) denotes that each RB in the pico eNB is only allocated to one pico UE; Eq. (13) means that each subframe is only classified as either the normal subframe or the protected subframe; the sum of $\varepsilon[i]$and $\varepsilon^{*}[i]$ for a particular subframe i is equal to 1; Eq. (14) implies that one pico UE can only be in the normal UE set or the protected UE set.

This resource allocation considered in this paper contains two main challenges: (a) *configuration of the ABS pattern*, i.e. determines the values of $\varepsilon[i]$ and $\varepsilon^{*}[i]$; and (b) *design of pico UE grouping*, i.e., determines the values of $C_{k^{''}}$ and $C_{k^{''}}^{*}$. So far, there is no research for considering these two problems jointly. We first consider the design of the ABS pattern, including how many protected subframes per ABS pattern should be configured in the system and which subframes should be configured as protected subframes. In this paper, we will present a joint solution for this resource allocation problem to maximize the sum rate of the system while maintaining the fairness among UEs. The proposed scheme can achieve balance between the system performance and the computational complexity, further comprising (a) *an ABS pattern design in Section 3*; (b) *a Pico UE grouping design* in Section 4; and (c) *a joint allocation scheme* in Section 5. The ABS pattern determination is executed at the macro eNB while the UE grouping and the joint allocation is executed at the pico eNB. The backhaul signaling among eNBs is required for the communication of ABS patterns. The following is a summary of symbols used in the paper along with their explanations.

$G^{(\text{Pico})}_{k'',n,q}$	the channel gain between the pico eNB and the k''th pico UE on the qth subcarrier of the nth RB
$p^{(\text{Pico})}_{k'',n,q}$	the amount of power for the k''th pico UE on the qth subcarrier of the nth RB
$G^{(\text{Macro})}_{k'',n,q}$	the channel gain between the macro eNB and the k''th pico UE on the qth subcarrier of the nth RB
$p^{(\text{Macro})}_{k',n,q}$	the amount of power for the k'th macro UE on the qth subcarrier of the nth RB
$\varepsilon[i]$	the binary indicator. Subframe configuration
$r^{(\text{normal})}_{k'',n}$	the data rate for thek''th pico UE on the nth RB in the normal UE set
$r^{(\text{protected})}_{k'',n}$	the data rate for thek''th pico UE on the nth RB in the protected UE set
$\rho^{(\text{Pico})}_{k'',n}$	the binary indicator. RB assignment
$\Omega^{(\text{normal})}$	the normal UE set
$\Omega^{(\text{protected})}$	the protected UE set
$R^{(\text{normal})}_{k''}$	the sum of data rate for thek''th pico UE in the normal UE set
$R^{(\text{protected})}_{k''}$	the sum of data rate for thek''th pico UE in the protected UE set
$\overline{R}$	the average data rate
I	the number of subframes in one frame
J	the windows size which is the number of the frames in a PF period
$C_{k''}$	the indicators for the UE k'' assigned to the normal UE set
$C^{*}_{k''}$	the indicators for the UE k'' assigned to the protected UE set
$F^{(\text{Macro})}[i]$	denotes that the sum rate of all macro UEs in the ith subframe
$F^{(\text{Pico})}_{(\text{protected})}[i]$	denotes that the sum rate of pico UEs in the protected UE set in the ith subframe
$F^{(\text{Pico})}_{(\text{normal})}[i]$	denotes that the sum rate of pico UEs in the normal UE set in the ith subframe
$\alpha,\beta,\mu,\psi_{k''},\varphi_{k''},\zeta_{k''},\zeta_{k''},\lambda_{k''}$	non-negative Lagrangian multipliers
N	the number of resource block in a system
Q	the number of subcarriers per resource block

3 Proposed ABS pattern design

As mentioned in the introduction section, two important issues need to be considered for the design: (a) the number of the protected subframes per ABS pattern should be determined in the system and (b) which subframes should be categorized as protected subframes. The time-invariant channel during a subframe is assumed because of the slow time-varying channel [24]. Therefore, we would design the ABS pattern by using subframe as the processing unit. We assume that all RBs are available and shared among UEs. Initially, without considering the UE grouping and resource allocation in this design phase, the channel information of all subcarriers in each subframe toward two eNBs in an ABS period is used. Our goal is to compare the performance index of each subframe which would be determined as normal or protected. Three variables are defined as:

$$F^{(\text{Macro})}[i] = \sum_{k'=1}^{K'}\sum_{n=1}^{N}\sum_{q=1}^{Q}\Delta f\log_2\left(1+SINR^{(\text{Macro})}_{k',n,q}[i]\right); \tag{17}$$

$$F^{(\text{Pico})}_{(\text{normal})}[i] = \sum_{k''=1}^{K''}\sum_{n=1}^{N}\sum_{q=1}^{Q}\Delta f\log_2\left(1+SINR^{(\text{normal})}_{k'',n,q}[i]\right); \tag{18}$$

$$F^{(\text{Pico})}_{(\text{protected})}[i] = \sum_{k''=1}^{K''}\sum_{n=1}^{N}\sum_{q=1}^{Q}\Delta f\log_2\left(1+SINR^{(\text{protected})}_{k'',n,q}[i]\right); \tag{19}$$

where $F^{(\text{Macro})}[i]$denotes that the sum rate of all macro UEs in the ith subframe; $F^{(\text{Pico})}_{(\text{normal})}[i]$ denotes that the sum rate of pico UEs in the normal UE set in the ith subframe; $F^{(\text{Pico})}_{(\text{protected})}[i]$ denotes that the sum rate of pico UEs in the protected UE set in the ith subframe. Therefore, the aggregate sum rate can be rewritten as:

$$\max_{\varepsilon[i],\varepsilon^*[i]} \sum_{i=1}^{I}\left(\varepsilon[i]F^{(\text{Macro})}[i]+\varepsilon[i]F^{(\text{Pico})}_{(\text{normal})}[i]+\varepsilon^*[i]F^{(\text{Pico})}_{(\text{protected})}[i]\right) \tag{20}$$

where the objective function (20) is subject to Eqs. (9–10, 13); the maximization is achieved by considering the values of $\varepsilon[i]$and $\varepsilon^*[i]$ according to the channels of each subframe. By using an optimization technique, we obtain the Lagrangian function with the relaxation [35] as:

$$\begin{aligned} L[i] = &-\sum_{i=1}^{I}\varepsilon[i]F^{(\text{Macro})}[i]-\varepsilon[i]F^{(\text{Pico})}_{(\text{normal})}[i]-\varepsilon^*[i]F^{(\text{Pico})}_{(\text{protected})}[i] \\ &+\sum_{i=1}^{I}\alpha[i]\left(\sum_{k'\in K'}\sum_{n=1}^{N}\sum_{q=1}^{Q}p_{k',n,q}[i]-P^{(\text{Macro})}[i]\right) \\ &+\sum_{i=1}^{I}\beta[i]\left(\sum_{k''\in K''}\sum_{n=1}^{N}\sum_{q=1}^{Q}p_{k'',n,q,l}[i]-P^{(\text{Pico})}[i]\right) \\ &+\sum_{i=1}^{I}\mu[i](\varepsilon[i]+\varepsilon^*[i]-1) \end{aligned} \tag{21}$$

where $\alpha[i]$, $\beta[i]$, and $\mu[i]$ are non-negative Lagrangian multipliers. $\varepsilon[i]$ is initially relaxed to be assumed as a real-valued number, and it will be used to determine its binary value. After differentiating $L[i]$ with respect to $\varepsilon[i]$and $\varepsilon^*[i]$, respectively, we have

$$\partial L[i]/\partial \varepsilon[i] = F^{(\mathrm{Macro})}[i] + F^{(\mathrm{Pico})}_{(\mathrm{normal})}[i] - \mu[i] = 0 \tag{22}$$

and

$$\partial L[i]/\partial \varepsilon^*[i] = F^{(\mathrm{Pico})}_{(\mathrm{protected})}[i] - \mu[i] = 0. \tag{23}$$

Therefore, we can determine whether the ith subframe should be classified as the normal subframe or the protected subframe by considering the difference between Eq. (22) and Eq. (23).

$$\Delta F[i] = F^{(\mathrm{Macro})}[i] + F^{(\mathrm{Pico})}_{(\mathrm{normal})}[i] - F^{(\mathrm{Pico})}_{(\mathrm{protected})}[i]. \tag{24}$$

Based on the derived result, $\Delta F[i]$ implies that the sum rate difference of the ith subframe configured as the normal subframe or the protected subframe. If the value of $\Delta F[i]$ is greater than zero, the ith subframe is configured as the normal subframe because it may achieve higher sum rate. Otherwise, the ith subframe is categorized as the protected subframe. After the development of the configuration of an ABS pattern, the UE grouping design will be shown in the next section.

4 Proposed UE grouping strategy

The resource allocation problem in the view of frequency domain is considered, especially for pico UEs. An UE grouping strategy is developed based on an optimization technique to determine which pico UEs use either the normal subframes or the protected subframes. Besides, the issue of proportional fairness among UEs is also studied. In this section, by using the ABS pattern designed in the previous section, we develop a strategy to determine the pico UE grouping while considering the fairness among UEs. The pico UE grouping problem for the maximization of the sum rate of pico eNBs can be formulated by using the second and the third term of Eq. (8) as:

$$U^{(\mathrm{Pico})} = \max_{C_{k''},C^*_{k''}} \sum_{i=1}^{I}\sum_{k''=1}^{K''}\left\{\begin{array}{l}\frac{C_{k''}}{\overline{R}^{(\mathrm{Pico})}_{k''}[i]}\sum_{n=1}^{N}\rho^{(\mathrm{Pico})}_{k'',n}[i]r^{(\mathrm{normal})}_{k'',n}[i]\\ +\frac{C^*_{k''}}{\overline{R}^{(\mathrm{Pico})}_{k''}[i]}\sum_{n=1}^{N}\rho^{(\mathrm{Pico})}_{k'',n}[i]r^{(\mathrm{protected})}_{k'',n}[i]\end{array}\right\} \tag{25}$$

where the function (25) is subject to Eqs. (9–12, 14); when $C_{k''} = 1$ represents that UE k'' is assigned to the normal UE set; when $C^*_{k''} = 1$ represents that UE k'' is assigned to the protected UE set on the pico eNB. However, this optimization problem is NP-hard and has a high computational complexity [24]. In this paper, we would analyze the pico UE grouping problem by using an optimization technique. The optimization problem (25) is transformed into the dual domain by forming its Lagrangian dual with the relaxation [35]. The Lagrangian function is shown as:

$$\begin{aligned} L'[i] = &-\sum_{i=1}^{I}\sum_{k''=1}^{K''}\frac{1}{\overline{R}^{(\mathrm{Pico})}_{k''}[i]}\left(C_{k''}R^{(\mathrm{normal})}_{k''}[i] + C^*_{k''}R^{(\mathrm{protected})}_{k''}[i]\right)\\ &+\sum_{k''=1}^{K''}\psi_{k''}\left(\sum_{k'=1}^{K'}\rho^{(\mathrm{Macro})}_{k',n}[i]-1\right) + \sum_{k''=1}^{K''}\phi_{k''}\left(\sum_{k''=1}^{K''}\rho^{(\mathrm{Pico})}_{k'',n}[i]-1\right)\\ &+\sum_{k''=1}^{K''}\zeta'_{k''}\left(\sum_{k'\in K'}\sum_{n=1}^{N}\sum_{q=1}^{Q}p^{(\mathrm{Macro})}_{k',n,q}[i]-P^{(\mathrm{Macro})}[i]\right)\\ &+\sum_{k''=1}^{K''}\zeta_{k''}\left(\sum_{k''\in K''}\sum_{n=1}^{N}\sum_{q=1}^{Q}p^{(\mathrm{Pico})}_{k'',n,q}[i]-P^{(\mathrm{Pico})}[i]\right)\\ &+\sum_{k''=1}^{K''}\lambda_{k''}\left(C_{k''}+C^*_{k''}-1\right) \end{aligned} \tag{26}$$

where $\psi_{k''}$, $\phi_{k''}$, $\zeta_{k''}$, $\zeta'_{k''}$, and $\lambda_{k''}$ are non-negative Lagrangian multipliers for the constraints (9–12, 14). The optimal solution Eq. (25) is achieved when the value of Eq. (26) is maximized. Therefore, the expression of the parameter $C_{k''}$ and $C^*_{k''}$ should be derived, which implies one pico UE is assigned to one of the UE sets.

First, by setting the partial derivative of Eq. (26) with respect to $C_{k''}$ to zero, we have

$$\frac{\partial L'[i]}{\partial C_{k''}} = 0 \Rightarrow \sum_{i=1}^{I}\frac{1}{\overline{R}^{(\mathrm{Pico})}_{k''}[i]}\sum_{n=1}^{N}\rho_{k'',n,l}[i]r^{(\mathrm{normal})}_{k'',n,l}[i] - \lambda_{k''} = 0. \tag{27}$$

Then, according to Eq. (8), we can get

$$\sum_{n=1}^{N}\rho_{k'',n}[i]r^{(\mathrm{normal})}_{k'',n}[i] = R^{(\mathrm{normal})}_{k''}[i]/C_{k''}. \tag{28}$$

By Eqs. (27) and (28), we can get

$$C_{k''} = \sum_{i=1}^{I}R^{(\mathrm{normal})}_{k''}[i]/\left(\lambda_{k''}\overline{R}^{(\mathrm{Pico})}_{k''}[i]\right). \tag{29}$$

Similarly, by setting the partial derivative of Eq. (26) with respect to $C^*_{k''}$ to zero, we can get

$$C^*_{k''} = \sum_{i=1}^{I}R^{(\mathrm{protected})}_{k''}[i]/\left(\lambda_{k''}\overline{R}^{(\mathrm{Pico})}_{k''}[i]\right). \tag{30}$$

By taking $C_{k''}$ (29) and $C^*_{k''}$ (30) into Eq. (14), we obtain

$$\sum_{i=1}^{I}\left(R_{k''}^{(\text{normal})}[i]+R_{k''}^{(\text{protected})}[i]\right)/\left(\lambda_{k''}\overline{R}_{k''}^{(\text{Pico})}[i]\right)=1$$
$$\Rightarrow\lambda_{k''}=\sum_{i=1}^{I}\left(R_{k''}^{(\text{normal})}[i]+R_{k''}^{(\text{protected})}[i]\right)/\overline{R}_{k''}^{(\text{Pico})}[i]. \tag{31}$$

By taking the expression of $\lambda_{k''}$ (31) into Eq. (29) and Eq. (30), respectively, we obtain

$$C_{k''}=\sum_{i=1}^{I}\frac{R_{k''}^{(\text{normal})}[i]}{\overline{R}_{k''}^{(\text{Pico})}[i]}\cdot\sum_{i=1}^{I}\frac{\overline{R}_{k''}^{(\text{Pico})}[i]}{R_{k''}^{(\text{normal})}[i]+R_{k''}^{(\text{protected})}[i]} \tag{32}$$

and

$$C_{k''}^{*}=\sum_{i=1}^{I}\frac{R_{k''}^{(\text{protected})}[i]}{\overline{R}_{k''}^{(\text{Pico})}[i]}\cdot\sum_{i=1}^{I}\frac{\overline{R}_{k''}^{(\text{Pico})}[i]}{R_{k''}^{(\text{normal})}[i]+R_{k''}^{(\text{protected})}[i]}. \tag{33}$$

Therefore, we can determine UE k'' which is assigned to the normal UE set or the protected UE set by comparing the difference of $C_{k''}$ (32) and $C_{k''}^{*}$ (33) which are related to the data rate. The difference of $C_{k''}$ (32) and $C_{k''}^{*}$ (33) is defined as:

$$\Delta C_{k''}=C_{k''}-C_{k''}^{*}. \tag{34}$$

$\Delta C_{k''}$ is the indicator difference of the normal UE set and the protected UE set when UE k'' is assigned to them. If the value of $\Delta C_{k''}$ is more than zero, UE k'' should be assigned to the normal UE set; otherwise, UE k'' should be assigned to the protected UE set.

5 Proposed joint allocation scheme

In this section, the joint ABS configuration and UE grouping scheme is described to resolve the resource allocation problem while achieving high system performance and fairness among all UEs. The proposed scheme by utilizing the designed functions includes the designs of the ABS pattern, the pico UE grouping, and the RB allocation. The procedures of the proposed scheme are as follows:

The pico UE index is $k''\in\{1,\ldots,K''\}$.$i$and$j$ are the subframe index and frame index, respectively. (i,j)denotes the ith subframe of the jth frame. $\overline{R}_{k'}^{(\text{Macro})}[i]$ and $\overline{R}_{k''}^{(\text{Pico})}[i]$ are the average date rate of macro UE and pico UE, respectively. One starts from $j = 1$, $j\in\{1,\ldots,J\}$, J is the window size which is the number of the frames in a PF period.

Step 1: ABS Configuration. Start from$i = 1$,$i \in \{1,\ldots,I\}$, $I$is the number of subframes in one frame. Each subframe is determined as the normal subframe or the protected subframe in one frame. The designed function $\Delta F[i]$ (24) determines which subframes should be configured as protected subframes in one frame. In order to find a better ABS pattern, we may sort the values of the designed function (24) in a descending order. And then, the number of protected subframes is limited to an upper bound of ABS density [22]. Therefore, the ABS pattern for a frame would be configured.

Step 2: Pico UE Grouping. After the ABS pattern is configured for a frame, we will assign pico UEs to the normal UE set or the protected UE set and allocate the RBs for each subframe. The initial UE set is determined by using Eq. (1). Pico UEs which are handed over from macro eNB to pico eNB because of bias values are assigned to the protected UE set $\Omega^{(\text{protected})}$, i.e., $C_{k''}^{*}=1$. The others are assigned to the normal UE set $\Omega^{(\text{normal})}$, i.e., $C_{k''}=1$.

Step 3: RB Allocation, for $n = 1, \ldots, N$. After the protected UE set $\Omega^{(\text{protected})}$and the normal UE set $\Omega^{(\text{normal})}$are determined, the RB allocation of each subframe is performed. For the normal subframes, only pico UEs which are assigned to the normal UE set can use the RBs; similarly, the RBs in the protected subframes can only be used by UEs in the protected UE set. We assume that power is equally distributed to each RB in the view of base station. In the initial stage, equal power is assumed for each subcarrier of each UE. A simple strategy is to assign RBs to UEs with a higher value of data rate. Since it is the first run of the solution, a better solution is achieved after iterations by the proposed scheme.

For the macro UEs, the nth RB of the ith subframe is allocated to the k'th macro UE with the maximum value of the function:

$$\hat{k}'=\underset{k'\in\Omega^{(\text{Macro})}}{\arg\max}\left\{r_{k',n}^{(\text{Macro})}[i]/\overline{R}_{k'}^{(\text{Macro})}[i]\right\}. \tag{35}$$

The nth RB is assigned to the k'th macro UE denoted as $\rho_{k',n}^{(\text{Macro})}[i]=1$. For the pico UEs in the normal UE set, the nth RB of the ith subframe which belongs to the normal subframe is allocated to the k''th pico normal UE with the maximum value of the function:

$$\hat{k}''=\underset{k''\in\Omega^{(\text{normal})}}{\arg\max}\left\{r_{k'',n}^{(\text{normal})}[i]/\overline{R}_{k''}^{(\text{Pico})}[i]\right\}. \tag{36}$$

Similarly, for the pico UEs in the protected UE set, the nth RB of the ith subframe is allocated to the pico UE with the maximum value of the function:

$$\hat{k}^{''} = \underset{k^{''} \in \Omega^{(\text{protected})}}{\arg} \max\left\{ r_{k^{''},n}^{(\text{protected})}[i] / \overline{R}_{k^{''}}^{(\text{Pico})}[i] \right\}. \tag{37}$$

The *n*th RB is determined as $\rho_{k^{''},n}^{(\text{Pico})}[i] = 1$ for the $k^{''}$th pico UE. Repeat *Step 3* until all the RBs, for $n = 1, ..., N$, are allocated in the *i*th subframe; then, repeat the same process until $i = I$. The initial sum rate denoted as $U_{(\text{initial})}^{(\text{Pico})}$ is calculated according to Eq. (25).

*Step 4: Fast Adjustment***.** We would re-distribute pico UEs into the two UE sets by using $C_{k^{''}}$ (32) and $C_{k^{''}}^{*}$ (33) in a group basis. If the $k^{''}$th UE is assigned to the normal UE set, we can get the $C_{k^{''}}$ according to Eq. (32); then, we temporarily move the $k^{''}$th UE from the normal UE set to the protected UE set; and repeat *Step 3* to allocate the RBs for each subframe. We can get the $C_{k^{''}}^{*}$ according to Eq. (33). Similarly, if the $k^{''}$th UE is assigned to the protected UE set, the same approach is used to get $C_{k^{''}}$ and $C_{k^{''}}^{*}$. After that, $\Delta C_{k^{''}}$ (34) is obtained for each pico UE. The value of $\Delta C_{k^{''}}$ would be used to determine if the $k^{''}$th UE is re-assigned to the normal UE set or the protected UE set. If $\Delta C_{k^{''}} \geq 0$, the pico UE $k^{''}$ is assigned to the normal UE set; otherwise, the pico UE $k^{''}$ is assigned to the protected UE set.

$$\begin{cases} C_{k^{''}} = 1 \text{ and } k^{''} \in \Omega^{(\text{normal})} & , \text{ if } \Delta C_{k^{''}} \geq 0 \\ C_{k^{''}}^{*} = 1 \text{ and } k^{''} \in \Omega^{(\text{protected})} & , \text{ if } \Delta C_{k^{''}} < 0 \end{cases} \tag{38}$$

After the pico UE re-assignment, the updated UE sets, i.e., $\Omega^{(\text{normal})}$ and $\Omega^{(\text{protected})}$, are obtained. The sum rate $U^{(\text{Pico})}$ according to Eq. (25) is calculated correspondingly. If the value of $U^{(\text{Pico})}$ is larger than that of $U_{(\text{initial})}^{(\text{Pico})}$, the normal UE set $\Omega^{(\text{normal})}$ and the protected UE set $\Omega^{(\text{protected})}$ are updated. Then, update $U_{(\text{initial})}^{(\text{Pico})}$ as $U^{(\text{Pico})}$ and repeat *Steps 3–4* until the value of $U^{(\text{Pico})}$ is no more increased.

Step 5: Refinement Mechanism. Based on the result of the fast adjustment, the refinement mechanism is performed to exchange or move pico UEs between two UE sets on a per-UE basis. The main concept of the refinement mechanism is to re-assign only one UE to the normal UE set $\Omega^{(\text{normal})}$ or the protected UE set $\Omega^{(\text{protected})}$ in one iteration. In the exchanging operation, originally two pico UEs, e.g., *x*and*y*, are assigned to$\Omega^{(\text{normal})}$and$\Omega^{(\text{protected})}$, i.e., $x \in \Omega^{(\text{normal})}$ and$y \in \Omega^{(\text{protected})}$. After the exchanging operation, two pico UEs are exchanged between two pico UE sets, i.e., $y \in \Omega^{(\text{normal})}$ and $x \in \Omega^{(\text{protected})}$. In this fashion, two pico UEs are exchanged in each time and the number of pico UEs in each set is not changed. The sum rate (25) of all combinations is calculated correspondingly. The sum rate increment can be defined as:

$$\Delta U_{(\text{exchange})}^{(\text{Pico})} = \left\{ U_{s^{'}}^{(\text{Pico})} - U_{(\text{initial})}^{(\text{Pico})} \right\}_{s^{'} \in S^{'}} \tag{39}$$

where $S^{'}$ denotes all combination cases in the exchanging operation; $s^{'}$ is one of combination cases; $U_{s^{'}}^{(\text{Pico})}$ is the sum rate of the $s^{'}$th combination case. In the moving operation, one pico UE is moved from $\Omega^{(\text{normal})}$ to $\Omega^{(\text{protected})}$ or from $\Omega^{(\text{protected})}$ to$\Omega^{(\text{normal})}$. After moving, the corresponding sum rate (25) is calculated. The sum rate increment can be defined as:

$$\Delta U_{(\text{move})}^{(\text{Pico})} = \left\{ U_{s^{''}}^{(\text{Pico})} - U_{(\text{initial})}^{(\text{Pico})} \right\}_{s^{''} \in S^{''}} \tag{40}$$

where $S^{''}$ denotes all combination cases in the moving operation; $s^{''}$ is one of combination cases; $U_{s^{''}}^{(\text{Pico})}$ is the sum rate of the $s^{''}$th combination case. Among all combinations $S^{'} \cup S^{''}$, one combination with the maximum sum rate increment would be selected to perform the corresponding operation.

$$s^{*} = \arg \max_{s^{*} \in S^{'} \cup S^{''}} \left\{ \Delta U_{(\text{exchange})}^{(\text{Pico})} \right\} \cup \left\{ \Delta U_{(\text{move})}^{(\text{Pico})} \right\}. \tag{41}$$

Then, update the sets of $\Omega^{(\text{normal})}$ and $\Omega^{(\text{protected})}$ and the initial value $U_{(\text{initial})}^{(\text{Pico})}$. Repeat *Step 5* until no sum rate increment can be achieved.

Step 6: Update the average data rates$\overline{R}_{k^{'}}^{(\text{Macro})}[i]$and $\overline{R}_{k^{''}}^{(\text{Pico})}[i]$ for the current frame. The proposed joint scheme is ready to be performed for the next frame$j = j + 1$. Return to Step 1 until the window size of frames $j = J$ is met.

In summary, Fig. 2a is a flow chart of the proposed joint allocation scheme. The proposed joint allocation scheme is executed on a per frame duration basis. First, ABS configuration for a frame determines each subframe as the normal subframe or the protected subframe at the macro eNB. The periodicity is a frame basis. The current channel state information may not be instantly estimated, so that we can use the channel information in the previous frame to design the ABS pattern because of the slow time-varying channel application. After that, the information of ABS configuration exchanges through the X2 interface between the macro eNB and the pico eNB. The X2 interface would be ideal backhaul as the latency may be less than 2.5 μs [36]. Therefore, the predicted sum rate can be calculated in the proposed ABS pattern design. The backhaul signaling may comprise the channel information of Pico UEs and the ABS configuration. The proposed Pico UE

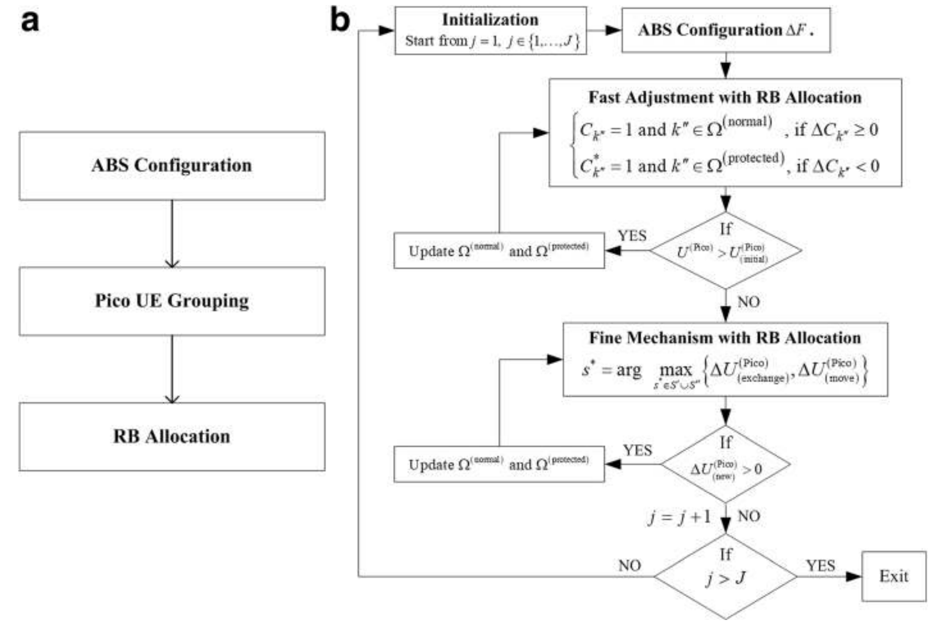

Fig. 2 **a** Flow chart of the proposed joint allocation scheme. **b** Procedures of the proposed joint allocation scheme

grouping strategy is performed locally for each subframe. i.e., pico UEs are assigned into two sets, i.e., the normal UE set or the protected UE set. In the step of Pico UE grouping, fast adjustment introduced in Section 4 and refinement mechanism in Section 5 are utilized to separate pico UEs into two groups for achieving better performance. The corresponding RB allocation in Section 5 is performed in the macro eNB and the pico eNB respectively. The proposed joint allocation scheme in Section 5 combines the above operations to maximize the sum rate of the system while maintaining the fairness among UEs.

We incorporate the computation and evaluation of related equations into Fig. 2a to complete the allocation procedures. Figure 2b illustrates the procedures of the proposed joint allocation scheme across the frequency domain and the time domain.

6 Computational complexity analysis

In this section, we focus on the computational complexity analysis of the RB allocation and UE grouping strategies in one frame in terms of Big-Oh notation. All compared schemes are based on the same system model, so the computational complexity of calculating the data rate associated with an SINR is the same, which is represented as $O(Q)$ by referring to Eq. (3) and Eq. (6). The complexities of the processing steps in the algorithm are the focus, in terms of calculating the SINR and the data rate.

Step 1 of the proposed joint allocation scheme is the ABS configuration for one frame. Regarding the proposed ABS pattern design, the calculation of the sum rate for each subframe in one frame is needed. Therefore, the complexity of the proposed ABS pattern design is $O(IK^{''}NQ)$. Step 2 uses Eq. (1) to determine the initial UE set. In that, $K^{''}$ UEs are considered which requires $O(K^{''})$. RB allocation is operated in *Step 3*. For the macro eNB, N RBs are considered for $K^{'}$ UEs per subframe. One frame contains I subframes. The computational complexity of the RB allocation needs $O(INK^{'}Q)$. For the pico eNB, we assume that $K^{''}$ UEs are equally distributed in each set. Each set needs the complexity of $O(INK^{''}Q/2)$ for the RB allocation. Therefore, $O(INK^{''}Q)$ is required for RA allocation of the pico UEs. *Step 4* focuses on the moving operation of the pico UEs. $K^{''}$ pico UEs are evaluated along with the RB allocation for one iteration. The complexity is calculated as $O((INK^{''}Q)K^{''}T_1)$. T_1 denotes the number of iterations. The refinement mechanism in *Step 5* comprises the exchanging operation and the moving operation. We also assume that the average number of pico UEs in each set is approximately $K^{''}/2$. For the exchanging operation, there are $(K^{''}/2) \cdot (K^{''}/2) \approx (K^{''})^2$ possible combinations per iteration. For the moving operation, the number of combinations is the number of total pico UEs $K^{''}$. Therefore, the complexity of the refinement mechanism along with the RB allocation is $O(INK^{''}Q((K^{''})^2 + K^{''})T_2) \approx O(IN(K^{''})^3QT_2)$. T_2 is the number of iterations. In summary, the complexity of the joint allocation scheme for one frame is $O(K^{''}INQ + K^{''} + INQ(K^{'} + K^{''}) + INQ(K^{''})^2T_1 + INQ(K^{''})^3T_2) \approx O(INQK^{'} + INQ(K^{''})^2T_1 + INQ(K^{''})^3T_2)$.

For the compared schemes, the computational complexity of the fixed ABS pattern [22] is $O(1)$ where it fixes the ABS density and determines an ABS pattern at random. Regarding pico UE grouping strategies, the full search scheme [25] is to search all UE grouping combinations of pico UEs in each ABS pattern. The complexity of all UE grouping combinations is $O\left(\sum_{j=1}^{K''} C_j^{K''}\right) \approx O\left(2^{K''}\right)$. So, the total computational complexity along with RB allocation is $O\left(INQK' + INQK'' \sum_{j=1}^{K''} C_j^{K''}\right) \approx O\left(INQK' + INQK'' 2^{K''}\right)$, including K' macro UEs and K'' pico UEs. $O(INQK')$ is the complexity of RA allocation for macro UEs. In [27], pico UE grouping is determined by CRE bias, which requires $O(K'')$. Therefore, the computational complexity along with RB allocation is $O(K'' + INQK' + INQK'')$. In [24], an indicator which involves the data rate is used to determine that each UE may be assigned to either the normal UE set or the protected UE set. The computational complexity of pico UE grouping is $O(K'' T_3)$. T_3 denotes the number of iterations. So, the total computational complexity along with RB allocation is $O(INQK' + INQK'' K'' T_3) = O(INQK' + INQ(K'')^2 T_3)$.

7 Simulation results

The simulation results will demonstrate the performance of the proposed scheme compared to those of the existing schemes [22, 24, 25, 27]. The network topology consists of one macro eNB and one pico eNB based on the 3GPP case 1 [37]. The radius of the macro eNB is 289 m, and the pico eNB is randomly distributed with a minimum distance of 75 m to the macro eNB. The frequency selective wireless channel model [38] is employed. We adopt Jake's model to generate the Rayleigh fading channel. The mobile speed is 4 km/h. The standard deviation of shadowing is 8 dB. $N_0$is −174 dBm/Hz. The channel power of the received signal for each UE is varied because of the various path losses at the different locations. The macro path loss model [39] is 128.1 + 37.6**log*(*d1*) in decibels. *d1* is in kilometers. The pico path loss model [39] is 38 + 30**log*(*d2*) in decibels. *d2* is in meters. The carrier frequency is 2 GHz. UEs are uniformly distributed within the coverage of the macro cell with the numbers from 12 to 36. Transmit power is 46 dBm for the macro eNB and 30 dBm for the pico eNB. Eight-decibel bias is considered for cell range expansion. The downlink FDD system is used for simulation with a bandwidth of 10 MHz comprising 50 RBs. Each RB has 12 subcarriers. Subcarrier spacing $\Delta f$is 15 kHz. The ABS pattern period is set to be 10 ms, i.e., 10-subframe duration. All results are the average values from 600 frames.

The first simulation is revealed to demonstrate the outperformance of the proposed ABS pattern design strategy. In order to have fair comparison, the fixed ABS approach is cooperated with a proper setting along with the proposed user grouping strategy and the proposed RB allocation scheme. The comparison baseline is the fixed ABS pattern method [22] with 50% ABS muting ratio, i.e., five ABS subframes per frame. The fixed ABS pattern [22] is also cooperated with the proposed user grouping strategy and the proposed RB allocation scheme. The result of Fig. 3 is conducted in the scenario with 24 UEs, which shows the results of the sum rates in the system versus different numbers of RBs. Figure 4 is conducted in the scenario with 50 RBs, which shows the results of the sum rates in the system versus different numbers of UEs. The simulation results indicate that the proposed ABS pattern design scheme outperforms the fixed ABS pattern method [22]. The enhancement is increased with the increment of the number of RBs because of more flexible resource scheduling. With user diversity, the performance is slightly improved with the number increment of UEs.

Based on the proposed ABS pattern design, the following simulation focuses on pico UE grouping strategies, including the full search scheme [25], the proposed joint allocation scheme, and the existing schemes [24, 27]. In Figs. 5 and 6, simulations are conducted in the scenario with 24 UEs at the bias value of 8 dB. In Fig. 5, it shows the results of the objective function (8) versus the number of RBs. It illustrates that the values of the objective function (8) are in the order of [Full search [23] > Proposed Joint Allocation Scheme > Ref. [24] > Ref. [27]] from large to small. The proposed joint allocation scheme approximates the full search scheme [25] while the computational complexity

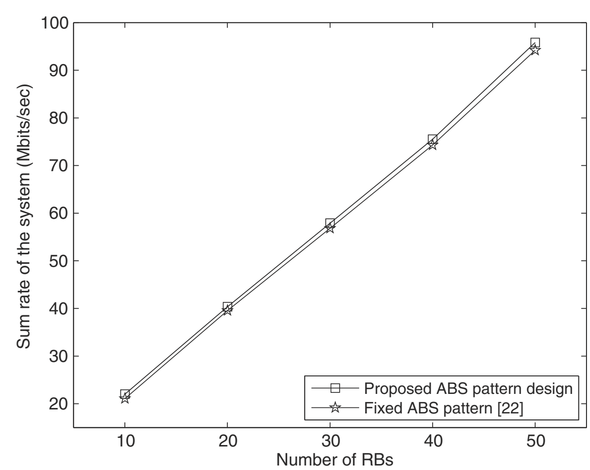

Fig. 3 Comparison of the proposed ABS pattern design with the fixed ABS pattern. The sum rate of the system versus the number of RBs with the number of UEs K = 24 and the bias value = 8 dB

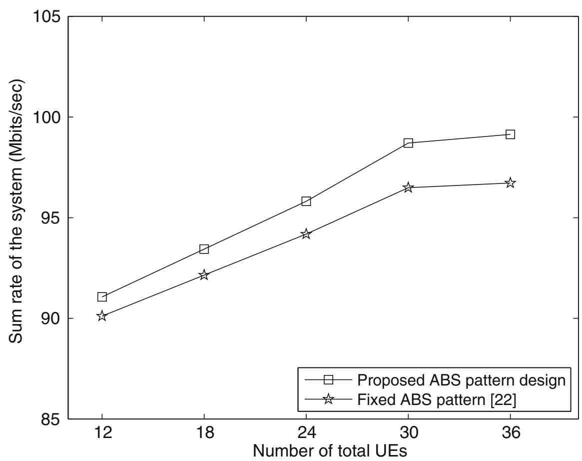

Fig. 4 Comparison of the proposed ABS pattern design with the fixed ABS pattern. The sum rate of the system versus the number of UEs with the number of RBs $N = 50$ and the bias value = 8 dB

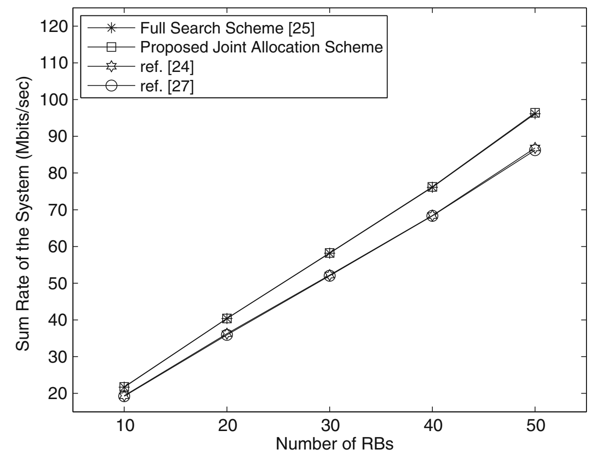

Fig. 6 Comparison of the sum rate of the system, in respect to Fig. 5

is greatly reduced. The simulation results also indicate that the proposed joint allocation scheme outperforms the existing schemes [24, 27]. Figure 6 shows the performance comparison in terms of the sum rate of the system. The simulation results indicate that the proposed joint allocation scheme still outperforms the existing schemes [24, 27]. The performance of the proposed joint allocation scheme is much closer to that of the full search scheme [25].

In Figs. 7 and 8, the simulations are in the scenario with 50 RBs by varying the number of total UEs. With the same performance trend, the proposed joint allocation scheme outperforms the existing schemes [24, 27] in terms of the objective function and the sum rate. The proposed scheme dynamically determines the pico UE grouping according to the functions (Eqs. 25 and 34), which would indicate the related rate performance of pico UEs. Thus, the proposed joint allocation scheme has better performance than the existing schemes [24, 27]. Compared to the full search scheme [25], the performance loss of the proposed joint allocation scheme is very tiny. Due to the multi-user diversity, the sum rate of the system is increased as the number of UEs increases. However, under the proportional fairness scheduler, the increase of the sum rate would become slow if the numbers of UEs are greater.

Figure 9 shows the fairness index (42). Jain's fairness index (FI) is a real number in the interval [33] denoted as

$$\mathrm{FI} = \left(\sum_{k''=1}^{K''} R_{k''}^{(\mathrm{Pico})}\right)^2 \Bigg/ \left(K'' \sum_{k''=1}^{K''} \left(R_{k''}^{(\mathrm{Pico})}\right)^2\right). \tag{42}$$

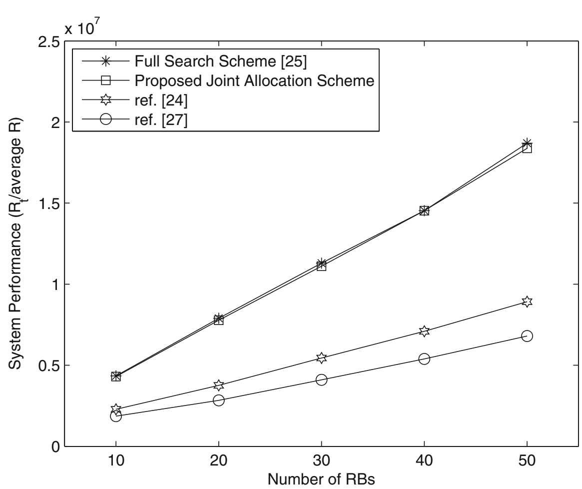

Fig. 5 Comparison of the proposed joint allocation scheme with the existing schemes. The value of the objective function versus the number of RBs with the number of UEs $K = 24$ and the bias value = 8 dB

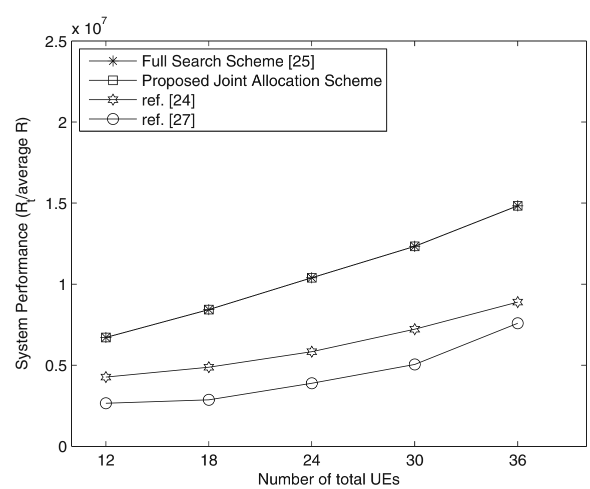

Fig. 7 Comparison of the proposed joint allocation scheme with the existing schemes. The value of the objective function versus the number of UEs with the number of RBs $N = 50$ and the bias value = 8 dB

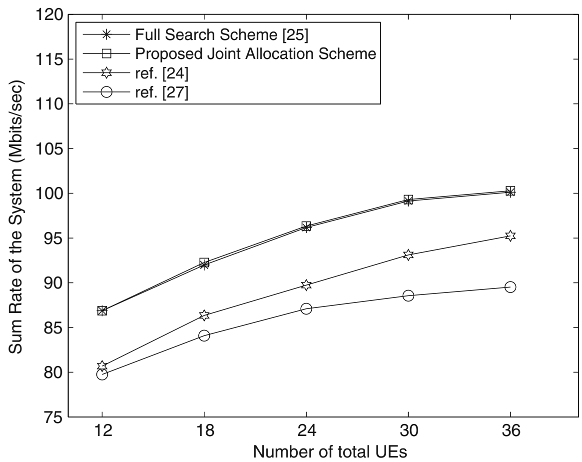

Fig. 8 Comparison of the sum rate of the system, in respect to Fig. 7

when FI = 1, it means that all UEs have the same performance with the highest fairness. When there are more UEs in the system, the fairness index would be descent. By considering the proportional fairness, the fairness index of the proposed joint allocation scheme would be almost equal to that of the full search scheme [25]. Note that the scheme [24] is designed to achieve the fairness of all UEs. Therefore, the value of the objective function would be better than that of the scheme [27] as shown in Figs. 5 and 7. Although slightly higher fairness is revealed as shown in Fig. 9, the sum rate is much worse than the proposed joint allocation scheme as shown in Figs. 6 and 8. From the results in Fig. 9, the difference between the scheme [24] and the proposed joint allocation scheme is negligible. Regarding the numbers of iterations required for the proposed joint allocation scheme and the existing scheme [24], almost the same numbers of iterations are revealed in our simulation. The average number of iterations is less than 6.

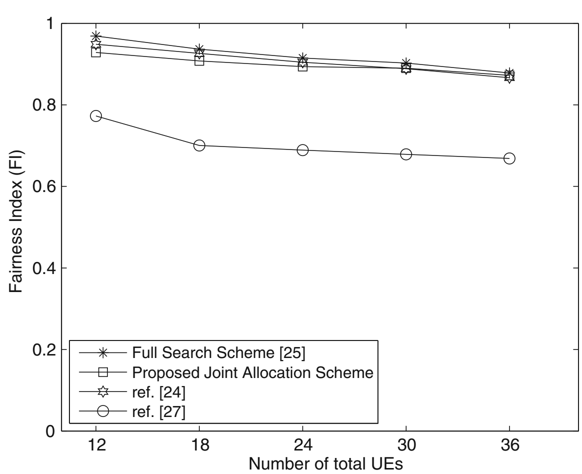

Fig. 9 Comparison of the fairness index, in respect to Fig. 7

8 Conclusions

A strategy with the help of the derived evaluation function to determine the ABS pattern is designed in this paper. With a proper design of ABS pattern, the performance would be further improved in term of sum rates. The novel UE grouping strategies are presented to improve the performance of the system without a prohibitive computational complexity. The proposed joint allocation scheme obtains the balance in the computational complexity and the performance, and also considers the fairness among UEs. The proposed joint allocation scheme outperforms the existing schemes about 10% gains in term of sum rate, and approaches 99.5% of the full search scheme while having a much lower complexity.

Acknowledgements
There is no other person who contributed toward the article who does not meet the criteria for authorship.

Funding
This work was supported by the Information and Communications Research Laboratories, Industrial Technology Research Institute (ITRI), Hsinchu, Taiwan, under Grant 2017–41–5G-0301.

Authors' contributions
W-CP is responsible for the development of the most parts of the algorithms and conducting simulations. J-WLin is responsible for the development of some parts of the algorithms and conducting simulations. Y-FC is responsible for the development of the algorithms, verification of the derivations and simulation results, writing the paper for the whole idea, and supervising the process of the research. C-LW is responsible for providing the whole concept of the algorithms to develop and supervising the process of the research. All authors read and approved the final manuscript.

Competing interests
The authors declare that they have no competing interests.

Publisher's Note

Author details
[1]Industrial Technology Research Institute, Zhudong, Taiwan, Republic of China. [2]Department of Communication Engineering, National Central University, Taoyuan, Taiwan, Republic of China. [3]Department of Electrical Engineering and Institute of Communications Engineering, National Tsing Hua University, Hsinchu, Taiwan, Republic of China.

Received: 7 October 2016 Accepted: 13 September 2017
Published online: 02 October 2017

References

1. E. Dahlman, S. Parkvall, J. Skold, *4G LTE/LTE-Advanced for Mobile Broadband* (Elsevier Ltd., UK, 2011)
2. *3GPP, Technical Specification Group Radio Access Network; Physical layer aspects for evolved Universal Terrestrial Radio Access (UTRA)*, TR 25.814, 2006
3. 3GPP, *Mobile Broadband Innovation Path to 4G: Release 9, Release 10 and Beyong: HSPA+, LTE/SAE and LTE-Advance,* 2010
4. 3GPP, *Requirements for further advancements for Evolved Universal Terrestrial Radio Access (E-UTRA) (LTE-Advanced)*, TR 36.913, 2011

5. 3GPP, *Further advancements for E-UTRA physical layer aspects*, TR 36.814, 2010
6. A. Khandekar, N. Bhushan, J. Tingfang, V. Vanghi, in *Proc. European Wireless Conf.* LTE-Advanced: heterogeneous networks (2011), pp. 978–982
7. A. Prasad, O. Tirkkonen, P. Lunden, O.N.C. Yilmaz, L. Dalsgaard, C. Wijting, Energy-efficient inter-frequency small cell discovery techniques for LTE-advanced heterogeneous network deployments. IEEE Commun. Mag. **51**(5), 72–81 (2013)
8. V. Chandrasekhar, J.G. Andrews, Femtocell networks: a survey. IEEE Commun. Mag. **46**(9), 59–67 (2008)
9. A. BouSaleh, S. Redana, B. Raaf, J. Hämäläinen, in *Proc. IEEE Vehicular Technology Conf.-Fall*. Comparison of relay and pico eNB deployments in LTE-advanced (2009), pp. 1–5
10. 3GPP, *Evolved Universal Terrestrial Radio Access (E-UTRA); Mobility enhancements in heterogeneous networks (Release 11)*, TR 36.839, 2012
11. R1-100701, in *3GPP TSG RAN WG1 Meeting#59*. Importance of Serving Cell Selection in Heterogeneous Networks (2010)
12. Y. Song, P.Y. Kong, Y. Han, Minimizing Energy Consumption through Traffic Offloading in a HetNet with 2-class Traffic. IEEE Commun. Lett. **19**(8), 1394–1397 (2015)
13. P.Y. Kong and G. K. Karagiannidis, "Backhaul-Aware Joint Traffic Offloading and Time Fraction Allocation for 5G HetNets", *IEEE Transactions on Vehicular Technology*, *DOI:* https://doi.org/10.1109/TVT.2016.2517671, 2016
14. A. Damnjanovic et al., A survey on 3GPP heterogeneous networks. IEEE Wirel. Commun. **18**(3), 10–21 (2011)
15. D. Luo, B. Li, D. Yang, in *Proc. IEEE Vehicular Technology Conf.-Fall*. Performance evaluation with range expansion for heterogeneous networks (2011), pp. 1–5
16. R1-112543, "Scenarios for eICIC evaluations," *3GPP TSG-RAN WG1 Meeting#66*, 2011
17. R1-106143, "Details of eICIC in macro-pico case," *3GPP TSG-RAN WG #63,* 2010
18. R1-110175, "Remaining issues of Rel-10 eICIC," *3GPP TSG-RAN WG1#63bis*, 2011
19. D. Lopez-Perez, I. Guvenc, G.D.L. Roche, M. Kountouris, T.Q.S. Quek, J. Zhang, Enhanced intercell interference coordination challenges in heterogeneous networks. IEEE Wirel. Commun. **18**(3), 22–30 (2011)
20. 3GPP, *Evolved Universal Terrestrial Radio Access (E-UTRA) and Evolved Universal Terrestrial Radio Access Network (E-UTRAN); Overall description; Stage 2 (Release 13)*, TS 36.300, 2015
21. J. Oh, Y. Han, in *Proc. IEEE Int. Symposium on Personal Indoor and Mobile Radio Commun*. Cell selection for range expansion with almost blank subframe in heterogeneous networks (2012), pp. 653–657
22. Y. Wang, K.I. Pedersen, in *Proc. IEEE Vehicular Technology Conf.-Spring*. Performance analysis of enhanced Inter-cell Interference Coordination in LTE-Advanced heterogeneous networks (2012), pp. 1–5
23. S. Deb, P. Monogioudis, J. Miernik, J.P. Seymour, Algorithms for enhanced Inter-cell Interference Coordination (eICIC) in LTE HetNets. IEEE/ACM Trans. Networking **99**, 1 (2013)
24. L. Jiang, M. Lei, in *Proc. IEEE Int. Symposium on Personal, Indoor and Mobile Radio Commun*. Resource allocation for eICIC scheme in heterogeneous networks (2012), pp. 448–453
25. J. Pang, J. Wang, D. Wang, G. Shen, Q. Jiang, J. Liu, in *Proc. IEEE Wireless Commun. and Networking Conf.* Optimized time-domain resource partitioning for enhanced inter-cell interference coordination in heterogeneous networks (2012), pp. 1613–1617
26. R1-100142, "*System performance of heterogeneous networks with range expansion*," *3GPP TSG-RAN WG1 Meeting#59bis*, 2010
27. R1-112411, "*Scenarios for further enhanced non ca-based icic for lte*," *3GPP TSG RAN WG1 Meeting#66*, 2011
28. A. Weber, O. Stanze, in *Proc. IEEE Int. Conf. Commun*. Scheduling strategies for HetNets using eICIC (2012), pp. 6787–6791
29. 3GPP, *Evolved Universal Terrestrial Radio Access (E-UTRA); Physical channels and modulation,* TR 36.211, 2011
30. 3GPP, *Evolved Universal Terrestrial Radio Access (E-UTRA); Physical layer – Measurements,* TR 36.214, 2010
31. H. Seo, B.G. Lee, in *Proc. IEEE Global Telecommun. Conf.* A proportional-fair power allocation scheme for fair and efficient multiuser OFDM systems, vol 6 (2004), pp. 3737–3741
32. H. Kim, Y. Han, A proportional fair scheduling for multicarrier transmission systems. IEEE Commun. Lett. **9**(3), 210–212 (2005)
33. V.D. Papoutsis, I.G. Fraimis, S.A. Kotsopoulos, User selection and resource allocation algorithm with fairness in MISO-OFDMA. IEEE Commun. Lett. **14**(5), 411–413 (2010)
34. R1-105406, in *3GPP TSG RAN WG1 meeting#62bis*. Support of time domain icic in rel-10 (2010)
35. S. Boyd, L. Vandenberghe, *Convex Optimization* (Cambridge University Press, 2004)
36. 3GPP, *Technical Specification Group Radio Access Network; Scenarios and requirements for small cell enhancements for E-UTRA and E-UTRAN (Release 12)*, TR 36.932, 2013
37. 3GPP, *Evolved Universal Terrestrial Radio Access (E-UTRA); Further advancements for E-UTRA physical layer aspects (Release 9)*, TS 36.814, 2010
38. L. Dong, G. Xu, H. Ling, in *Proc. IEEE Global Telecommun. Conf.* Prediction of fast fading mobile radio channels in wideband communication systems, vol 6 (2001), pp. 3287–3291
39. 3GPP, *LTE; Evolved Universal Terrestrial Radio Access (E-UTRA); Radio Frequency (RF) requirements for LTE Pico Node B,* TR 36.931, 2011